

On Performance Study of Solar Driven Heat Engine with Consideration to Internal Irreversibility and Power Density

Abhijit Sinha *, Agnimitra Biswas *[‡], KK Sharma*

* Department of Mechanical Engg., Research Scholar, National Institute of Technology Silchar

(abhinit05@gmail.com, agnibis@yahoo.co.in, kksharma1313@rediffmail.com)

[‡] Corresponding Author; Agnimitra Biswas, Department of Mechanical Engg., Research Scholar, National Institute of Technology Silchar, Silchar-788 010 (Assam), India, +91 3842 224879, agnibis@yahoo.co.in

Received: 22.04.2013 Accepted: 09.06.2013

Abstract- Finite time thermodynamic optimization with respect to maximum power density has been performed for a solar-driven heat engine with internal irreversibility. In this paper, it is considered that the heat transfer from the hot reservoir to the working fluid occurs in radiation mode and the heat transfer from working fluid to the cold reservoir occurs in the convection mode. The equation of power density function is formed, which is maximized for various design parameters. Further, the effects of these parameters on optimum power density is also investigated. Moreover, the performance in the nominal power density output at operating conditions other than optimum working fluid temperatures has been studied with respect to the obtained efficiency.

Keywords- Solar driven heat engine, performance analysis, internal irreversibility, power density, thermal efficiency.

1. Introduction

Finite time thermodynamics has recently been used off late for the performance analysis of a solar driven heat engine. The objective function chosen for optimization is usually power density output. Optimization studies for performance analysis of heat engines using finite time thermodynamics were firstly done by Chambadal [1] and Novikov [2]. Curzon and Ahlborn [3] analysed the performance of an endoreversible Carnot heat engine under maximum power output condition. Over the last few years, some works on power optimization of heat engines with consideration to endoreversible and irreversible models have been reported in the existing literature [4]. Goktun et al. [5] studied the performance of endoreversible radiative heat engine at maximum power output conditions. That work was extended for irreversible radiative model by Ozkaynak [6]. Analysis of carnot heat engine based on endoreversible condition with combined radiation & convection between the engine and the hot/cold heat reservoirs was performed by Erbay & Yavuz [7]. Study on power optimization of endoreversible solar driven carnot engine model was carried

out by Badescu et al. [8]. Following this many researchers [9-11] performed optimization of solar driven endoreversible carnot engine by taking specific power output (power output/area) as the optimization criterion. The pioneering work on finite time thermodynamic analysis for a solar driven heat engine was done by Sahin [12]. The optimum operating conditions for the heat engine at maximum power condition was reported in that paper. Further Sahin et al. [13-15] optimized the performances of an endoreversible Carnot heat engine and reversible/irreversible Joule-Brayton heat engines using the power density as a criterion.

Koyun [16] compared the performances of a solar-driven heat engine under maximum power and maximum power density conditions with consideration to external irreversibilities.

In this paper, the performance of optimum work density has been investigated for different design parameters. Also performance in the nominal power density output at operating points other than optimum working fluid conditions with variation in efficiency for various parameters have also been investigated. In this paper,

specific engine size as area ratio between hot reservoir and cold reservoir, extreme temperature ratios between the hot & cold side reservoirs have been considered as the necessary design parameters

2. The Theoretical Model

Reversible Carnot cycle is the basis in the development of classical thermodynamics. The reversible Carnot cycle as upper performance bound is the idealised cycle in which it is required that the system be passed through a series of quasi static equilibrium states, which is also considered in the present analysis. The T-S diagram of the present reversible solar-driven heat engine with consideration to internal irreversibilities is shown in Fig.1.

The heat engine works between two extreme temperatures (T_H and T_L). Assuming heat transfer from hot reservoir (T_H) to the working fluid occurs in radiation mode, then the heat transfer, Q_H from the hot reservoir to the heat engine can be written as

$$\dot{Q}_H = C_H A_H (T_H^4 - T_X^4) \tag{1}$$

The heat transfer, Q_L from the heat engine to the cold reservoir (T_L), with an assumption of being in convection mode, can be written as

$$\dot{Q}_L = C_L A_L (T_Y - T_L) \tag{2}$$

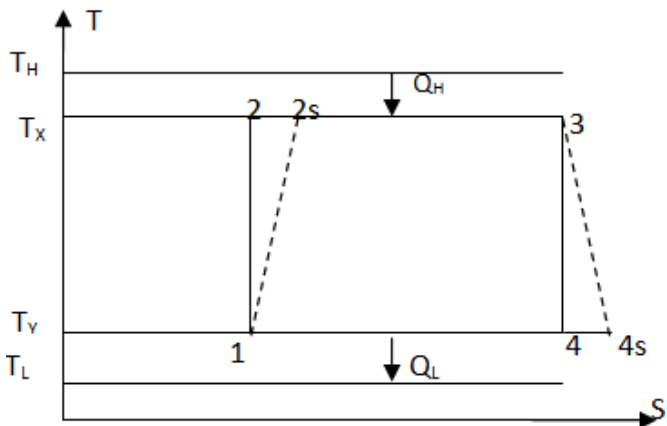


Fig.1. T-S diagram of a reversible solar-driven heat engine with internal irreversibility

In the above two equations, CH and CL are the heat transfer coefficients of the hot and cold fluids respectively. By the first law of thermodynamics, the output power (W) from the cycle can be represented as-

$$\dot{W} = \dot{Q}_H - \dot{Q}_L = C_H A_H (T_H^4 - T_X^4) - C_L A_L (T_Y - T_L) \tag{3}$$

Now the expression for thermal efficiency becomes

$$\eta = 1 - \frac{\dot{Q}_L}{\dot{Q}_H} = 1 - \frac{C_L A_L (T_Y - T_L)}{C_H A_H (T_H^4 - T_X^4)} \tag{4}$$

By the assumption of ideal gas, the maximum volume in the cycle V₄ is represented as

$$V_4 = \frac{mRT_4}{P_4} \tag{5}$$

In equation 5, ‘m’ is mass of the working fluid and ‘R’ is universal gas constant. Here, the pressure in the cycle at the minimum point (P4) is assumed to be constant. Power density, defined as the ratio of power to the maximum volume in the cycle [14–15], is the performance parameter for the present analysis. This can thus be represented as:

$$\dot{W}_d = \frac{\dot{W}}{V_4} = \frac{C_H A_H (T_H^4 - T_X^4) - C_L A_L (T_Y - T_L)}{\frac{mRT_4}{P_4}} \tag{6}$$

By the second law of thermodynamics, for an irreversible cycle, the resultant variation in the entropy of the working fluid under heat addition and heat removal gives:

$$\int \frac{\partial \dot{Q}}{T} = \frac{\dot{Q}_H}{T_X} - \frac{\dot{Q}_L}{T_Y} < 0 \tag{7}$$

One can rewrite the inequality in Equation (7) as

$$\frac{\dot{Q}_H}{T_X} = I \frac{\dot{Q}_L}{T_Y}, \quad 0 < I < 1 \tag{8}$$

With the above definition I becomes

$$I = \frac{\dot{Q}_H T_Y}{\dot{Q}_L T_X} = \frac{T_X (s_3 - s_2) T_Y}{T_Y (s_4 - s_1) T_X} = \frac{s_3 - s_2}{s_4 - s_1}$$

Substituting equation (1) & (2) in equation (8), we have

$$T_Y = \frac{T_L}{1 - \frac{C_H A_H (T_H^4 - T_X^4)}{C_L A_L T_X}} \tag{9}$$

where, Ar = AH/AL= ratio of area of hot reservoir to cold reservoir = specific engine size

I = internal irreversibility

Substituting equation (9) in (4) & (6), the thermal efficiency, dimensionless power density output

$$\bar{W}_d = \frac{\dot{W}_d}{C_L A_L \frac{P_4}{mR}} \text{ can be expressed as}$$

$$\eta = 1 - \frac{\tau}{I\theta - A_r x (1 - \theta^4)} \tag{10}$$

$$\bar{W}_d = \frac{A_r x (1 - \theta^4) (I\theta - A_r x (1 - \theta^4) - \tau)}{I\theta\tau} \tag{11}$$

where, θ = TX / TH = working fluid temperature ;

τ = extreme temperature ratio = TL / TH ;

x = temperature constant = CHTH3 / CL

To find the optimum working fluid temperature under maximum power density, equation (11) is differentiated with respect to θ and the resulting derivative is set to zero as

$$7Arx^2 + 4ArI^2 - (6x + 3\tau)Ar - Ar(\tau + x) = 0 \quad (12)$$

The optimum values of θ have to satisfy Equation. (11) for maximum power density outputs. The solution of these equations can be done numerically.

3. Results and Discussion

The variations of the optimum power density (W_{dmax}) with respect to area ratio between hot side and cold side reservoirs, i.e specific engine size (A_r) for various extreme temperature ratios, τ is shown in fig.2. W_{dmax} values first increase with A_r , but as A_r becomes high they decrease for all τ . Further it is observed that with the increase in τ values, the optimum power densities decrease for all values of A_r . And it is close to zero when $\tau = 0.6$.

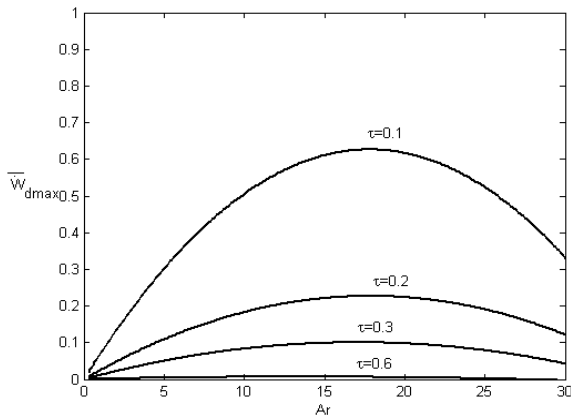


Fig. 2. Variation of optimum power density with respect to area ratio for different τ values ($x = 0.01, I=0.9$)

Figure 3 shows the variations of the optimum power density (W_{dmax}) with area ratio between hot side and cold side reservoirs (A_r) for various values of the temperature constant 'x'. It can be seen from the figure that as the value of x increases, the optimum power density increases but the interval of A_r in which the power density gets maximum drops as x increases. The best zone of operation would be $A_r < 5$ when x is kept at 0.9 as can be seen from the figure. The typical values of x for solar-driven heat engine applications are expected to be on the order of 1, or even less [16].

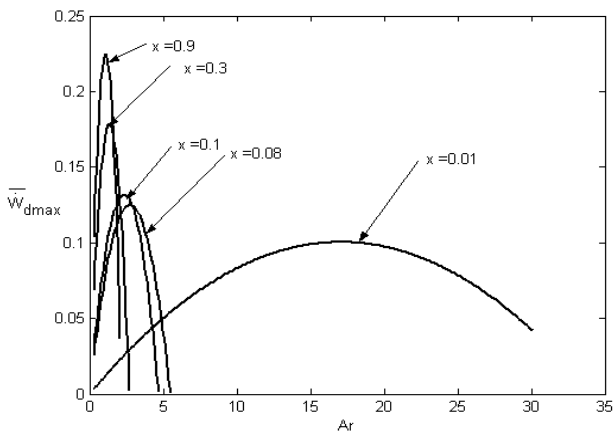


Fig. 3. Variations of optimum power density with respect to area ratio for selected values of x ($\tau=0.3, I=0.8$)

The variations of the optimum power density (W_{dmax}) as function of area ratio between hot side and cold side reservoirs (A_r) for various irreversibility factors (I) is shown in fig. 4. There has been a quick rise in the power density values for A_r up to 10 for all values of I, but after that as A_r increases further, the power densities decrease.

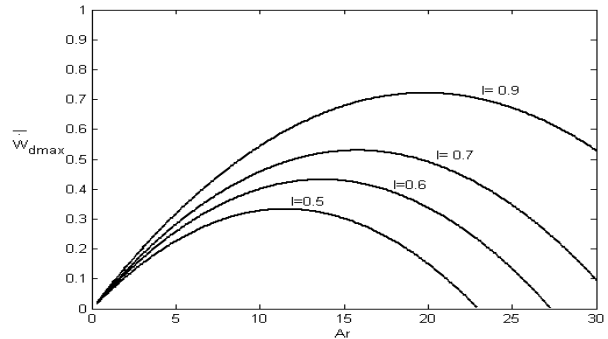


Fig. 4. The variation of optimum power density with respect to area ratio for different irreversibility values, I ($x=0.01, \tau=0.1$)

Further, as internal irreversibilities increase (i.e, $I \ll 0.9$), optimum power densities decrease for all values of A_r . In fig. 5, the variations of nominal power density output other than optimum working fluid temperature conditions with respect to thermal efficiency is shown for different values of the temperature constant x. The nominal outputs get high values in the operating efficiency range of 40-50%. Thus other than optimum condition of efficiency, high values of outputs can be obtained by operating in that efficiency range. Further, operating in that range, the nominal power density outputs can be increased by using high values of the constant x up to 1.0 as can be seen from fig. 5.

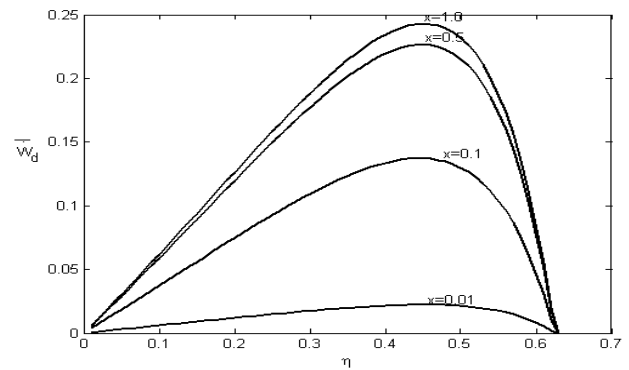


Fig.5. Variation of nominal power density with respect to thermal efficiency for different x values ($I= 0.8, \tau = 0.3$ & $A_r = 2$)

In Fig. 6, variations of nominal power density other than optimum working fluid temperature conditions with respect to thermal efficiency is shown for different values of area ratio, A_r . The nominal power density outputs get high values in the operating efficiency range 40-50%. Thus other than optimum condition of efficiency, high values of outputs can be obtained by operating in that efficiency range when A_r is the important design parameter under consideration. Further, being in that range, the nominal outputs can be increased by keeping high values of A_r .

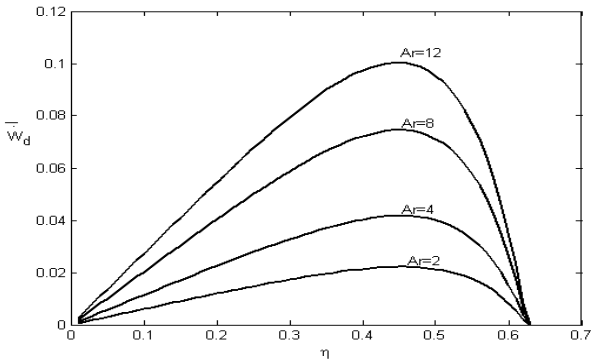


Fig 6. Variations of nominal power density with respect to thermal efficiency for different values of A_r ($I = 0.8, \tau = 0.3$ & $x = 0.01$)

The variations of nominal power density output other than optimum conditions with respect to thermal efficiency for different values of irreversibility factors I is shown in fig. 7. It is observed that efficiencies at maximum values of nominal power density outputs decrease with the increase in internal irreversibilities(i.e, when $I < 0.9$) For engine as reversible as $I = 0.9$, better performance in nominal power density output can be obtained in the efficiency range 50-60% as can be seen from fig. 7.

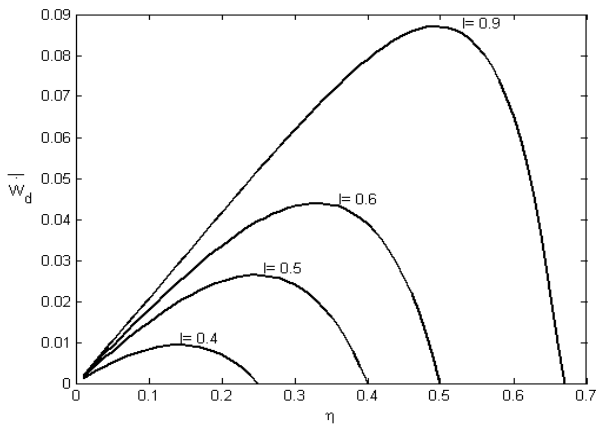


Fig.7. Variation of power density output with thermal efficiency for different values of I ($A_r = 8; \tau = 0.3; x = 0.01$)

The variations of nominal power densities with respect to thermal efficiency for different values of extreme temperature ratio, τ is shown in fig. 8. The efficiencies at maximum values of nominal power density outputs decrease with the increase in the extreme temperature ratio, τ . The nominal work densities decrease as τ increases for the whole operating range of thermodynamic efficiency. Further as can be seen from fig. 8, minimum work density output is obtained when $\tau = 0.6$.

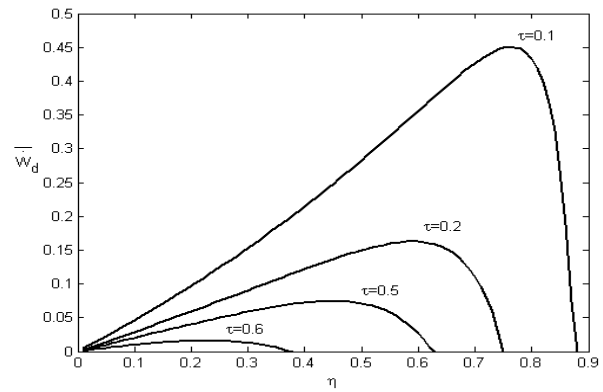


Fig. 8. Variation of power density with thermal efficiency for different values of τ ($A_r = 2; I = 0.8; x = 0.01$)

In figures 9,10,11, variations of optimum efficiencies for maximum power density output have been studied with respect to the specific engine size (area ratio between the reservoirs) for different values of I, τ & x respectively. The optimum thermal efficiency values stay high for $A_r < 5$ for all values of I , but as A_r crosses that mark, the optimum efficiencies decrease. Further maximum values of optimum efficiency can be obtained by keeping irreversibilities as low as $I = 0.9$ for all A_r . But if A_r is more than 15 units, high efficiency outputs decrease even if irreversibilities are low. The results are equivalent to the findings in the variation of optimum power density output with respect to the area ratio, A_r for the corresponding values of I and τ as shown in figures 2 & 4 previously. There, the optimum power densities stayed high low values of A_r under same values of I & τ and then dropped with increase in A_r .

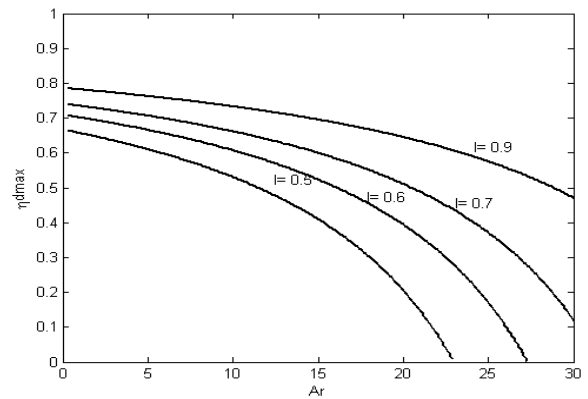


Fig.9. Variation of efficiency at max. power density with respect to area ratio for different irreversibility values ($x = 0.01, \tau = 0.1$)

In the variation of η_{dmax} for different values of x , it is found that η_{dmax} decreases sharply in the range $A_r < 5$ for $x = 0.08$ up to $x = 0.9$. It is only when $x = 0.01$ that efficiency drops slowly with A_r until it is only 10% when $A_r = 30$. This result is also equivalent to the variations in max power density with respect to A_r for the corresponding values of x where maximum work density outputs have been obtained in $A_r < 5$ when x is kept up to 0.9.

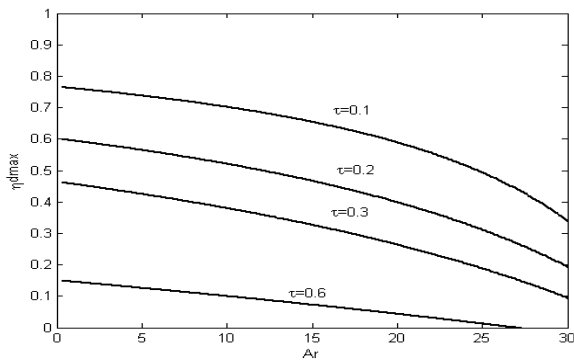


Fig.10. Variation of efficiency at max. power (work) density with respect to area ratio for different τ values ($x=0.01$, $I=0.9$)

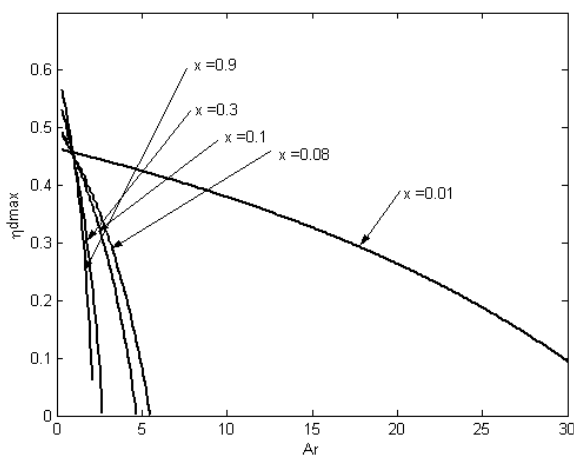


Fig.11. Variations of optimum efficiency at max. power density with respect to area ratio for different values of x ($\tau=0.3$, $I=0.8$)

4. Conclusion

A performance analysis of solar driven heat engine with internal irreversibility has been done in the present study. It is observed that maximum optimized power density outputs depend on design parameters. It has been found that for better performance in W_{dmax} , low values of extreme temperature ratio, τ and low values of area ratio A_r , and high values of irreversibility factors should be employed. The effects of design parameters on nominal work density output have also been investigated in this paper. Further, the variation of optimum efficiencies corresponding to the maximum power densities with respect to area ratio for different parameters like τ , I , x etc have also been studied. The results of finite time thermodynamics and endoreversibility are entirely equivalent to the same case analyzed by a classical reversible Carnot cycle with internal irreversibility of heat transfer. However more investigations may be required to arrive at concrete conclusions for the study been made.

References

- [1] Chambadal P. Les Centrales Nucleaires. Paris: Armond Colin; 1957. p. 41–58.
- [2] Novikov II. The efficiency of atomic power stations (a review). *Atom Energy* 1957; 3(11):409.
- [3] Curzon FI, Ahlborn B. Efficiency of a Carnot engine at maximum power output. *Am J Phys* 1975; 43:22–4.
- [4] Bejan A. Entropy generation minimization: the new thermodynamics of finite-size devices and finite-time processes. *Appl Phys Rev* 1996;79:1191–218.
- [5] Goktun S, Ozkaynak S, Yavuz H. Design parameters of a radiative heat engine. *Energy* 1993; 18:651–5.
- [6] Ozkaynak S. Maximum power operation of a solar powered heat engine. *Energy* 1995; 20:715–21.
- [7] Erbay LB, Yavuz H. An analysis of an endoreversible heat engine with combined heat transfer. *J Phys D:Appl Phys* 1997; 30:2841–7.
- [8] Badescu V. Optimum design and operation of a dynamic solar power system. *Energy Convers Manage* 1996; 37:151–60.
- [9] Wu C. Power optimization of an endoreversible Brayton gas turbine heat engine. *Energy Convers Mgmt* 1991;31:561–5.
- [10] Chen J, Wu C. General performance characteristics of an n-stage endoreversible combined power cycle at maximum specific power output. *Energy Convers Mgmt* 1996;37:1401–6.
- [11] Chen J, Wu C, Kiang RL. Maximum specific power output of an irreversible radiant heat engine. *Energy Convers Mgmt* 1996;37:17–22.
- [12] Sahin AZ. Optimum operating conditions of solar driven heat engines. *Energy Convers Manage* 2000; 41:1335–43.
- [13] Sahin B, Kodal A, Yavuz H. Maximum power density for an endoreversible Carnot heat engine. *Energy* 1996;21:1219–25.
- [14] Sahin B, Kodal A, Yavuz H. Efficiency of Joule–Brayton engine at maximum power density. *J Phys D:Appl Phys* 1995;28:1309–13.
- [15] Sahin B, Kodal A, Yılmaz T, Yavuz H. Maximum power density analysis of an irreversible Joule–Brayton engine. *J Phys D:Appl Phys* 1996;29:1162–7.
- [16] Koyun A. Performance analysis of a solar driven heat engine with external irreversibilities under maximum power and power density condition. *Energy Convers Manage* 2004; 45:1941–7.